# A NOVEL CONTEXTUAL SPECKLE REDUCTION METHOD OF POLSAR IMAGES: EVALUATION OF SPECKLE REDUCTION EFFECTS ON SEA ICE CLASSIFICATION

M. Mahdianpari*
B. Salehi
F. Mohammadimanesh
Department of Electrical Engineering
C-CORE and Memorial University of Newfoundland
Captain Robert A. Bartlett Building
Morrissey Road, St. John's, NL, Canada A1B3X5
m.mahdianpari@mun.ca
bahram.salehi@c-core.ca
f.mohammadimanesh@mun.ca

## ABSTRACT

Polarimetric Synthetic Aperture Radar (PolSAR) sensors can transmit and receive electromagnetic waves in different polarization states. As a result, PolSAR images are complex multi-dimensional data which can be extensively applied in sea ice monitoring and classification. The discrimination capability of PolSAR data makes them a unique source of information with a significant contribution to make in tackling problems concerning environmental applications, especially in the Arctic regions. The increasing temperature of the Earth due to climate change, combined with the degradation of ice thickness in the Arctic region increases the navigation of shipping routes more than ever before. Thus, oil and gas resources at high latitudes are more accessible, which will increase economic activities in the Arctic. Therefore, sea ice monitoring is one of the most important applications of remote sensing tools, since it is time and cost efficient in comparison with extensive field campaigns.

Speckle reduction is one of the most important pre-processing steps in Polarimetric Synthetic Aperture Radar (PolSAR) image processing. This paper demonstrated the importance of the de-speckling method for sea ice classification using PolSAR image. A novel contextual speckle reduction method was proposed based on the integration of a Markovian energy function as a contextual analysis, and the Gaussian model as a pixel-wise analysis which maintained the mean value of original data in the homogenous areas and preserved the edges of features in the heterogeneous regions. Our proposed method is applied to a full polarimetric L-band dataset, ALOS-1 PALSAR acquired from Baffin Bay. The efficiency of the proposed method was compared with other well-known de-speckling methods, such as the Kuan method, the enhanced Lee method, and the Nonlocal Means and Refined Lee method. Different de-speckling indices, including the Mean Square Error (MSE), the Signal to Noise Ratio (SNR), the Edge Saving Index (ESI), and Equivalent Number of Looks (ENL) were extracted for filtered images from different methods. Moreover, the capability of all de-speckled PolSAR images was compared in terms of overall sea ice classification results. The results demonstrated that the proposed method was outperformed by other well-known methods in terms of both de-speckled indices as well as classification results.

**KEYWORDS:** Polarimetric Synthetic Aperture Radar (PolSAR), Compact Polarimetric (CP), Sea ice Classification, Speckle reduction, Markov Random Field (MRF).

## INTRODUCTION

Sea ice is simply frozen ocean water that covers an extensive area in both the Arctic and Antarctica regions (Ochilov and Clausi, 2012). Sea ice has an important role in a variety of environmental processes, including global temperature, movement of ocean water, the freezing process, heat exchange and circulation. Importantly, it is the only habitat for a number of arctic creatures such as the polar bear. Furthermore, significant oil and gas resources are found within the arctic region, which highlights the importance of ship navigation during all seasons. Despite the benefits, the sea ice environment is being degraded at an increasing rate due to global warming. A reduction of multi-year sea ice which is being replaced with seasonal (new) sea ice type can be seen as a serious threat for this environment. Thus, the sustainable management of this important ecosystem is an important environmental issue.

One traditional and still currently used approach for sea ice monitoring is daily ice charts. These charts illustrate the best estimation of ice conditions using a variety of data resources, such as satellite imagery, aircraft or ship-based observations. However, the classification of a large number of images by trained experts is time- and cost-consuming, which may not be accurate enough due to human errors.

The advances in remote sensing tools for the classification of complex land cover environments has integrated with Polarimetric Synthetic Aperture Radar (PolSAR) images and significantly changed sea ice classification and monitoring in the past decades (Scheuchl et al., 2005). Particularly, the unique capability of SAR signals to operate independently of weather and day/night conditions has helped them become the main source of data for the operational recognition and the monitoring of sea ice, either in the context of manual sea ice charts or advanced automated remote sensing classification. Also, SAR signals have the advantage of penetrating into ice surfaces, which provides information about ice structure and its composition. Thus, in recent years, an automated sea ice classification system has gained increasing attention (Scheuchl et al., 2005; Karvonen et al., 2005; Ochilov and Clausi, 2012). However, the main problem with PolSAR images is speckle noise, which degrades the radiometric quality of images and, accordingly, affects the accuracy of PolSAR data end products. Speckle is a signal granular noise with a multiplicative model, which affects the coherent imaging radar system. In this realm, an affective speckle reduction approach significantly improves the quality of SAR image processing. Particularly, the quality of PolSAR processed images, such as classification, segmentation, and target detection significantly depends on the accuracy and reliability of the PolSAR input data. Thus, speckle reduction is one inevitable preprocessing step in PolSAR image processing. During the last three decades, several speckle reduction methods have been proposed (Novak and Burl, 1990; Lopes et al., 1993; Xie et al., 2002; Mahdianpari et al., 2012).

Most of the traditional de-speckling approaches have assumed statistical independency from the original image and speckle. Particularly, the ratio of the standard deviation to the mean was considered to be constant in speckle (Lee et al., 1994). Lee, Kuan, and Frost filters are a number of well-known traditional de-speckling filters, which have utilized a weighted averaging approach for estimating of the local statistical parameters in the spatial domain (Lee, 1981; Frost et al., 1982; Kuan et al., 1987). Later, Lee et al. (2009) introduced an adaptive Lee filter, which mitigated the problem of the original Lee filter. Particularly, it has been developed based on the Minimum Mean Square Error (MMSE), and applied to a target signature preservation technique in order to overcome the problem of noisy edge boundaries associated with the original Lee filter (Lee et al., 2009). The nonlocal (NL) filtering approach is another category of de-speckling approaches based on the concept of data-driven weighted averaging. The main idea is pixel weighting according to the similarity of the target pixel with the reference pixel. A relatively recent comprehensive study focusing on different SAR speckle reduction techniques is found in Argenti et al., (2013).

An effective SAR de-speckling method should address four main criterions including: (1) speckle reduction in homogeneous areas; (2) edge and texture perseveration in heterogeneous areas; (3) radiometric preservation, which means that an efficient de-speckling filter should not introduce bias on reflectivity; and (4) absence of artefacts

(Argenti et al., 2013). An assessment of the speckle reduction method is one of the most challenging tasks. This is because the noise-free reflectivity that we would like to obtain is unknown. In the last decade, several quality assessment indices have been proposed, which are mainly divided into with-reference and without-reference indices. In this study, a number of without-reference indices were used to evaluate the effectiveness of the proposed method. However, a practical approach for evaluating the effectiveness of a de-speckling method is to assess the success of subsequent processing tasks; for example, the overall classification accuracy obtained by a de-speckled PolSAR image.

In this study, we proposed a new speckle reduction method for PolSAR imagery based on an adaptive Gaussian Markov Random Field (GMRF) model. The adaptive nature of the proposed method causes the suppression of speckle noise, while preserving details and edges. The de-speckled PolSAR image was then utilized for complex sea ice classification using a supervised Maximum Likelihood Classifier (MLC) (Richards, 1999). In particular, we evaluated the effects of the proposed method and three other well-known filters, including the Kuan method, the enhanced Lee method, and the Nonlocal mean and refined Lee method in a comparative framework on the overall classification results. The proposed method has been applied to a full polarimetric ALOS PALSAR-1 image from Baffin Bay, Newfoundland and Labrador, Canada.

## CASE STUDY AND DATASET

An ascending full polarimetric ALOS PALSAR-1 image acquired on May 25th, 2007 with an incident angle of about 23.86° was used for this study. The study area is located at the north east portion of Baffin Bay, which is a marginal sea of the North Atlantic Ocean. Baffin Bay is a semi-enclosed ocean basin between Greenland and Baffin Island that connects the Arctic Ocean and the North West Atlantic, providing an important economic pathway for the exchange of heat, salt, and oil and gas resources between these 2 oceans (Hamilton and Wu, 2013). This area is characterized by a typical severe Arctic climate with frequent storms, experiencing an average temperature of 7℃ in July and -20℃ and -28℃ in the southern and northern part in January, respectively. The mean annual precipitation ranges from 100 to 250mm on the Greenland side and about twice as much near Baffin Island. Figure 1 depicts the geographic location of the study area with satellite image overlay.

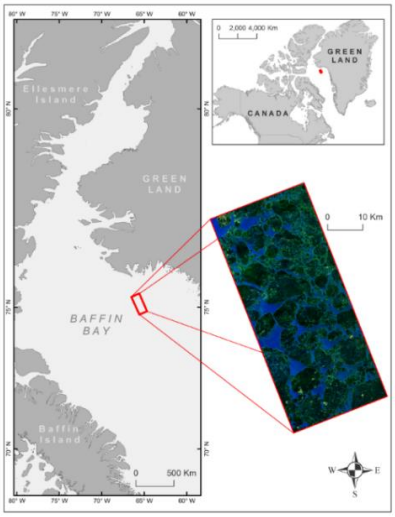


**Figure 1.** The geographic location of the study area. The red box denotes ALOS PALSAR coverage.

## METHODOLOGY

The phase fluctuations of the returned electromagnetic (EM) signals make the appearance of the PolSAR image grainy. The speckle has a multiplicative model in a SAR image, which is formulated as follows:

$$I(x) = R(x)v(x) \tag{1}$$

where $I(x)$ denotes the noisy image, $R(x)$ is the pure radar backscatter of ground targets and $v(x)$ represents the speckle noise. Therefore, one of the main factors that reduce the performance of further PolSAR image analysis is the signal-dependent speckle noise. In this study, an adaptive approach based on Markov Random Fields (MRFs) under the Hammersley-Clifford theorem was used to define the energy function in order to reduce speckle noise. A global optimization algorithm, the simulated annealing (SA), was then applied to minimize the energy function for speckle reduction. The results of different de-speckling methods were evaluated by several quantitative matrices, including the mean-square error, SNR, an edge-preservation parameter, and the equivalent number of looks (ENL). The de-speckled PolSAR images with different methods were then inserted into a Maximum Likelihood Classification algorithm. We further assessed the effect of different de-speckling methods on the result of sea ice classification. A detailed description of each step is presented in the following sections.

### Contextual Speckle Reduction

A MRF model presents a spatial correlation between neighboring pixels and has been utilized in this study in order to both extract contextual information and integrate contextual and pixel-wise information. In the case of image processing, MRF theory enables the modeling of contextual dependencies between a set of sites S, which are given by:

$$S = \{s = (i, j); 1 \leq i \leq M, 1 \leq j \leq N\} \tag{2}$$

The sites can be pixels in an image or individuals in a social network. A random field value is defined by S as follows:

$$\Gamma = \{\gamma_s, \gamma_s \in B, s \in S\} \tag{3}$$

where B denotes the pixel lattice and sets of all possible values in the image. The values for a set of sites S will be denoted by:

$$X = \{x_1, x_2, x_3, \ldots x_n\} \tag{4}$$

Figure 2 depicts the first and second-order neighborhood systems.

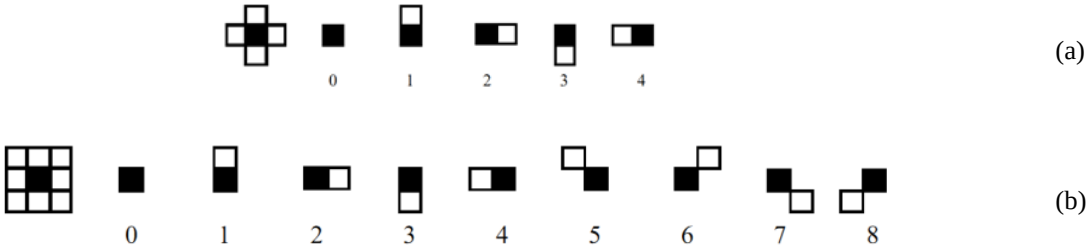


**Figure 2.** (a) First-order neighborhood system and its division into cliques. The black squares represent the site of interest and the white squares represent the neighboring sites. (b) Second-order

neighborhood system and its division into cliques.

The index 0 in both neighboring systems denotes the single clique and other indices are pair-cliques. The Conditional Probability Density Function (CPDF) of the label at a site that is derived from the labels of the neighboring sites is given by:

$$p(x_i|x_j) = \frac{\exp\left(-\frac{\left|\mu\left(r_{x_i x_j}\right)\right|^2 x_i + x_j}{I_j\left(1-\left|\mu\left(r_{x_i x_j}\right)\right|^2\right)}\right)}{I_j\left(1-\left|\mu\left(r_{x_i x_j}\right)\right|^2\right)} \psi_0\left(\frac{2(x_i x_j)^2\left|\mu\left(r_{x_i x_j}\right)\right|}{I_j\left(1-\left|\mu\left(r_{x_i x_j}\right)\right|^2\right)}\right) \quad (5)$$

where $I_j$ denotes the true intensity image at point j, and $\left|\mu\left(r_{x_i x_j}\right)\right|$ and $r_{x_i x_j}$ represent the coherence factor and the Euclidian distance between points I and j, respectively. $\psi_0(.)$ is a modified Bessel function of the first kind and zero order. The coherence factor is defined as:

$$\left|\mu\left(r_{x_i x_j}\right)\right| = \begin{cases} \left|\alpha_{r_{x_i x_j}}\right| \in [0,1[ & \forall\, r_{x_i x_j} \leq 1 \\ 0 & Otherwise \end{cases} \quad (6)$$

To estimate the probability density function, the MRF energy function is defined as follows:

$$p_X(x) = \exp[-U(x)] = V_{C_1}(x) + V_{C_2}(x) \quad (7)$$

where $V_{C_1}$ and $V_{C_2}$ denote the single-clique and the pair-clique potential functions. This energy function was used for the speckle reduction procedure in this study.

## Quantitative indices

In this study, four different quantitative indices were used to evaluate the performance of the proposed method, as well as other well-known methods in term of speckle reduction in PolSAR images and the preservation of image information.

Mean Square Error (MSE)

The MSE value presents the difference between the original and the de-speckled image and is formulated as follows:

$$MSE(\hat{I}, R) = E[(\hat{I} - I)^2] \quad (8)$$

where $\hat{I}$ and $I$ are the de-speckled and original image, respectively.

Signal to Noise Ratio (SNR)

The SNR index is one of the widely used parameter for de-speckling evaluation and is formulated as follows:

$$SNR = 10 \log \left(\sum_{j=1}^{k} I_i^2 / \sum_{j=1}^{k} (I_i - \hat{I}_i)^2\right) \quad (9)$$

Edge Saving Index (ESI)

The Edge Saving Index (ESI) evaluates the edge-saving ability of the de-noising algorithm in the horizontal (ESI_H) and vertical (ESI_V) directions. The formulae are computed from (10) and (11) as follows:

$$ESI\_H = \frac{\sum_{m=1}^{M} \sum_{n=1}^{N-1} \left|\hat{I}_{m,n+1} - \hat{I}_{m,n}\right|}{\sum_{m=1}^{M} \sum_{n=1}^{N-1} \left|I_{m,n+1} - I_{m,n}\right|} \quad (10)$$

$$ESI\_V = \frac{\sum_{m=1}^{M-1} \sum_{n=1}^{N} \left|\hat{I}_{m+1,n} - \hat{I}_{m,n}\right|}{\sum_{m=1}^{M-1} \sum_{n=1}^{N} \left|I_{m+1,n} - I_{m,n}\right|} \quad (11)$$

Equivalent Number of Looks (ENL)

ENL is an index that represents the ability of the de-speckling method and the efficiency of the smoothing procedure (Lee et al., 2015):

$$ENL = \frac{E(\hat{I})}{Var(\hat{I})} \quad (12)$$

where $E(\hat{I})$ and $Var(\hat{I})$ are the mean and standard deviation of the de-speckled image, respectively. Higher values of ENL show a greater filter efficiency in de-speckling procedures.

### Maximum Likelihood Classifier (MLC)

A supervised ML classification was carried out for this study. Training samples were selected and sorted using daily ice charts corresponding to the date of PolSAR image acquisition (25/05/2007). In addition to open water class, two other land cover classes, including thin first year ice and thick first year ice existed in the PolSAR image based on a daily ice chart. First year ice is characterized as sea ice of not more than one winter's growth. Thin first year ice is 30-50cm thick, while the thick first year ice is greater than 120cm. After selecting polygons representing the training dataset, a MLC was performed. Given n-dimensional data, the MLC calculates the probability$L_i(x)$, wherein pixel x belongs to a specific class $W_i$ as follows:

$$L_i(x) = \ln p(w_i) - \frac{1}{2}\ln|\Sigma_i| - \frac{1}{2}\,(x - m_i)^T \Sigma_i^{-1} (x - m_i) \quad (13)$$

where $p(w_i)$is the same for all classes and defined as a probability that class $w_i$occurs in the data. $\Sigma_i$ and $m_i$ are the covariance matrix and mean of class $w_i$. The superscript $T$ denotes the transpose operation (Richards, 1999).

## RESULT AND DISCUSSION

Different de-speckling methods, including the Kuan method, the enhanced Lee method, the Nonlocal Means and Refined Lee method, as well as the proposed method were applied to three diagonal elements of the coherency matrix. Fig. 3 illustrates the de-speckled PolSAR image using different methods. For better evaluation of de-speckling performance a zoomed area was selected with different sea ice types representing both homogeneous area and edges.

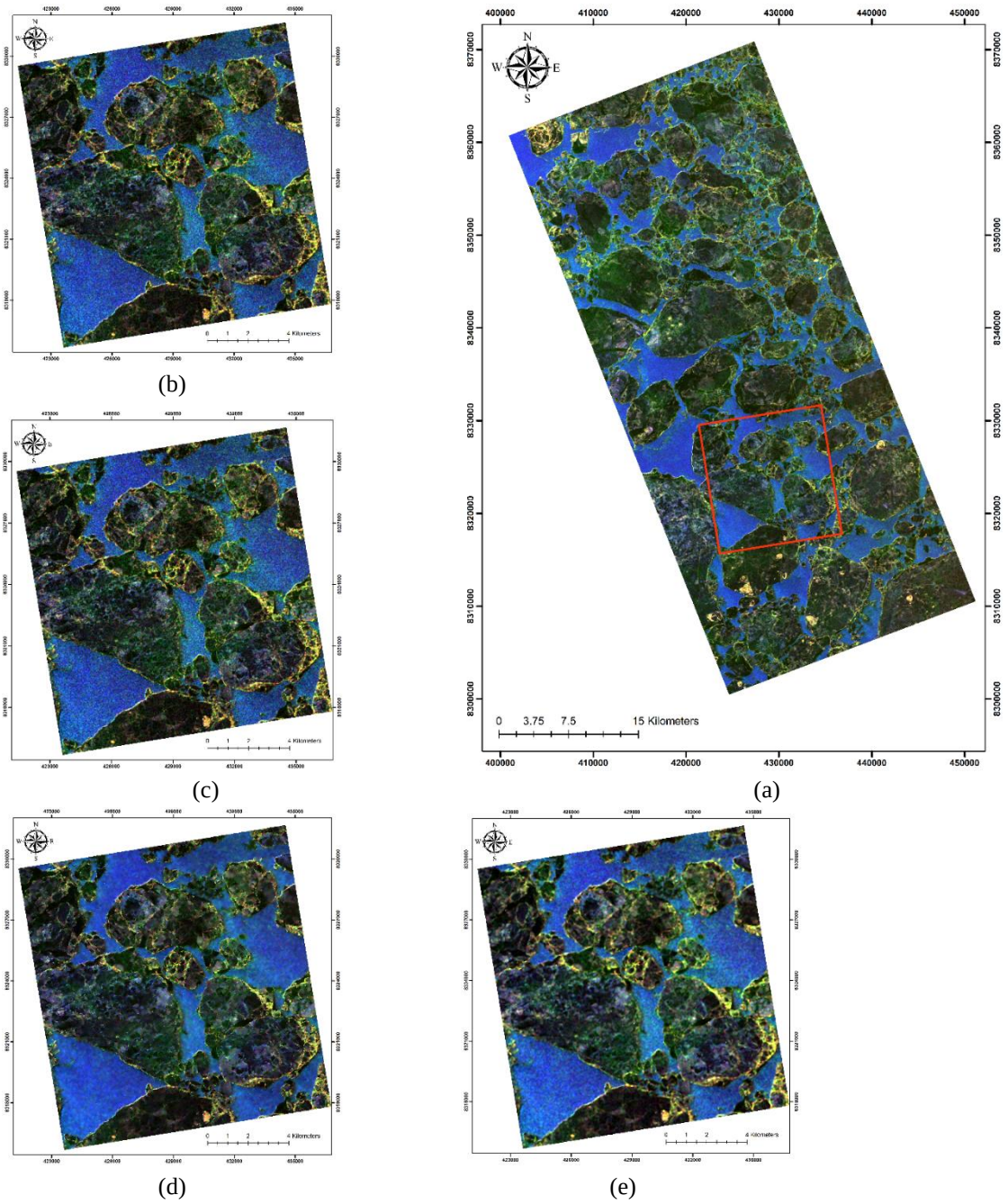


**Figure 3.** The de-speckled images: (a) the proposed method, (b) the Kuan method, (c) the Enhanced Lee method, (d) the Nonlocal Means and Refined Lee method, and (e) the zoomed image of the proposed method.

As seen, even when using well-known de-speckling approaches such as Kuan and Enhanced Lee, a large amount of speckle noise still remained (see Fig. 3 (b) and (c)). The Nonlocal Means and Refined Lee method was

more successful for removing speckle compared to the first two de-speckling filters, though it was less successful in preserving the mean value of the original image (Fig. 3 (d)). The proposed method proved to be the most successful de-speckling method in terms of both removing speckle and maintaining the mean value of the original image.

Fig. 4 illustrates the performance of different de-speckling methods in terms of the MSE index.

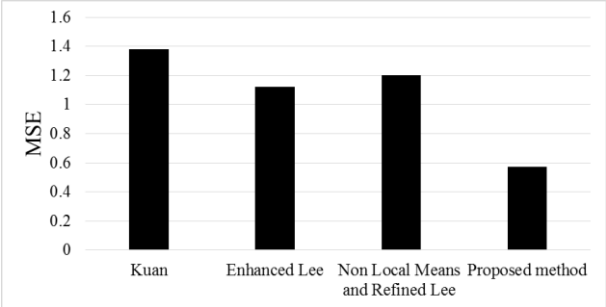


**Figure 4.** Comparing Mean Square Error (MSE) between different de-speckling methods.

The MSE parameter represents the global assessment of de-speckling performance. As seen in Fig. 4, the Kuan and proposed method represented the highest and lowest MSE. In particular, a MSE of about 1.39, 1.1, 1.19, and 0.58 were obtained by the Kuan, Enhanced Lee, Nonlocal, and the proposed method, respectively. Thus, the proposed method demonstrated a better ability for preserving the mean of the original signal compared to other methods. Another de-speckling assessment conducted in this study was Signal-to Noise Ratio (SNR). Fig.5 illustrates SNR values for different de-speckling methods.

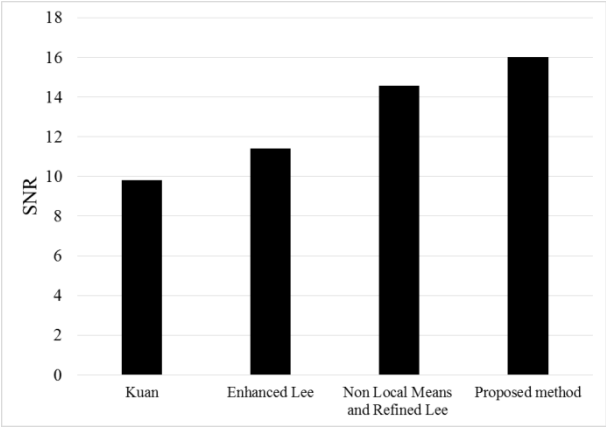


**Figure 5.** Comparing Signal to Noise Ratio (SNR) between different de-speckling methods.

As seen, the proposed method attained the highest SNR value in comparison with other filters. More precisely, a SNR value of about 15.9, 14.3, 11.3, and 9.7 was obtained by the proposed method, Nonlocal, Enhance Lee, and Kuan filter, respectively. Again, the Kuan filter was shown to be the least successful filter with a lower SNR value than other filters. We also evaluated the capability of different de-speckling methods in terms of the edge preservation index. Table 1 shows the result of different de-speckling methods in terms of the edge saving index.

**Table 1.** The efficiency of different filters in term of edge preservation in both horizontal and vertical directions.

| De-speckling methods | ESI-H | ESI-V |
|---|---|---|
| Kuan | 0.41 | 0.43 |
| Enhanced Lee | 0.64 | 0.66 |
| Nonlocal Means and Refined Lee | 0.58 | 0.61 |
| Proposed method | 0.65 | 0.69 |

The results illustrated that both the proposed method and the enhanced Lee method were successful for edge preservation in horizontal and vertical directions. However, the proposed method demonstrated a slightly better capability. The nonlocal filter method also showed comparable results with the first two successful filters.

Finally, we examined the performance of de-speckling methods in terms of ENL values. Fig. 6 depicts the ENL values for different filters in this study.

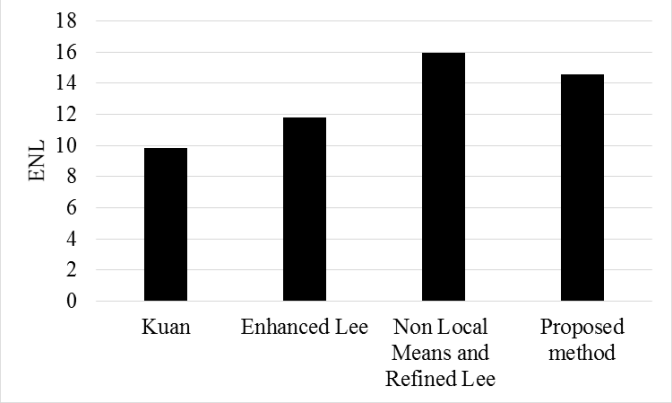


**Figure 6.** Comparing the Equivalent Number of Look (ENL) for different de-speckling methods in this study.

This index evaluates the degree of smoothing in homogeneous areas. As seen, the Nonlocal filter illustrated the highest ENL value, which indicated the highest degree of smoothing as compared to other filters. The Kuan and Enhanced Lee filter demonstrated the lowest ENL values. This was also observed in Fig. 3, wherein a large amount of speckle noise remained even after applying these two filters (Fig. 3 (b), (c)).

The proposed method represented the intermediate level of smoothing according to Fig. 6.

Next, all de-speckled images using different de-speckling methods were applied into a supervised ML classifier. Particularly, we evaluated the capability of different de-speckling methods for improving the overall classification accuracy. Table 2 illustrates the overall classification results obtained by different de-speckled images in this study.

**Table 2.** Overall Accuracy (OA) and Kappa coefficient obtained by de-speckled images from different filters.

| De-speckling methods | OA (%) | K |
|---|---|---|
| Kuan | 61 | 0.49 |
| Enhanced Lee | 68 | 0.54 |
| Nonlocal Means and Refined Lee | 64 | 0.51 |
| Proposed method | 79 | 0.68 |

As seen in Table 2, the proposed method and the enhanced Lee method resulted in the highest overall classification accuracies. However, the overall accuracy for the proposed method was 11% higher than the enhanced Lee method. The overall classification accuracy obtained by the Kuan filter image was the lowest. The result demonstrated the importance of an efficient de-speckling method for PolSAR image processing. Fig. 7 depicts the most significant classified map obtained by the proposed method.

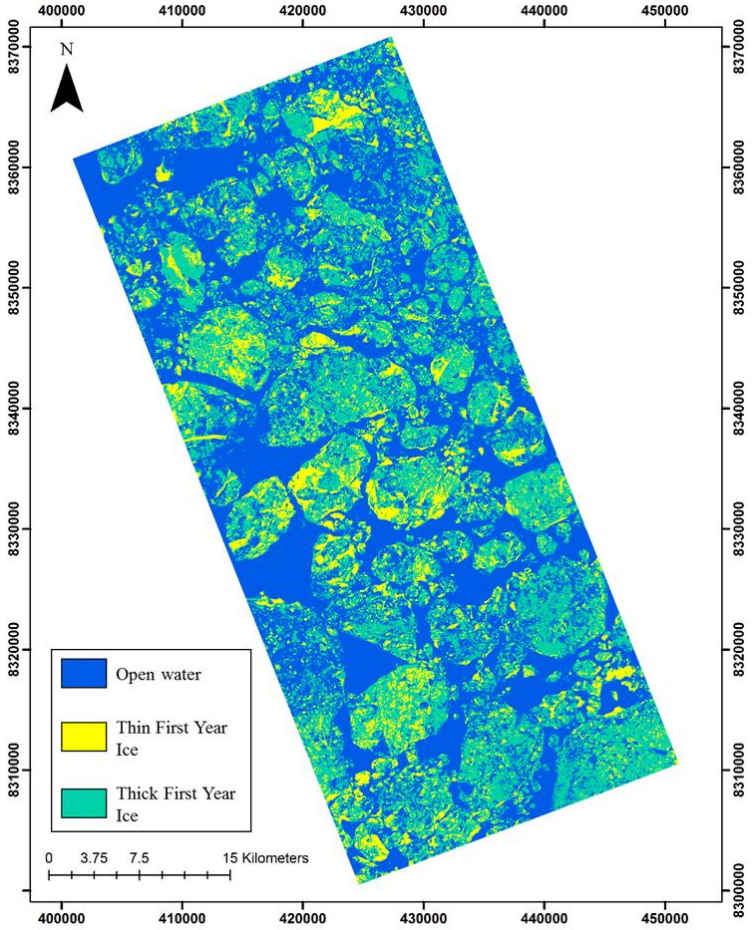


**Figure 7.** The most significant classified map obtained by de-speckled image based on the proposed method, which illustrated an overall classification of about 79%.

The classified map has three classes, including open water, thin first year ice, and thick first year ice. The classified map illustrates a detailed distribution of different sea ice classes. Table 3 represents the confusion matrix of the most significant results, which have been obtained by the proposed method.

**Table 3.** The confusion error matrix for the most significant result in this study, which was obtained by the de-speckled image based on the proposed method.

| | Open Water | Thin First year ice | Thick First year ice | User Acc. (%) |
|---|---|---|---|---|
| Open Water | 13067 | 1145 | 687 | 87.70 |
| Thin First year ice | 471 | 5049 | 1925 | 67.82 |
| Thick First year ice | 97 | 1953 | 6201 | 75.15 |
| Prod. Acc. (%) | 95.83 | 61.97 | 70.36 | |

The open water class represented the highest user's and producer's accuracy, which illustrated the least omission and commission error. In contrast, the thin first year ice class represented the lowest user's and producer's accuracy, which demonstrated the highest omission and commission error for this class. Overall, confusion error was observed between thin and thick first year ice.

## CONCLUSIONS

In this study, we evaluated the importance of an efficient de-speckling method for improving PolSAR image processing. Particularly, a new de-speckling method based on an adaptive Gaussian Markov Random Field (GMRF) model was proposed, and its efficiency was evaluated compared to other well-known de-speckling methods, including the Kuan method, the enhanced Lee method, and the Nonlocal Means and Refined Lee method. Several de-speckling indices were used to evaluate the capability of the proposed method as well as other methods. Overall, the proposed method proved to be more efficient in terms of both mean signal preservation and speckle reduction. Particularly, the de-speckled images obtained by the Kuan and enhanced Lee methods exhibited signs of noise after applying the filter. Although, the Nonlocal Means and Refined Lee method was better able to remove noise, it was still unsuccessful in mean signal preservation. The de-speckled PolSAR images were further used in the Maximum Likelihood Classifier for sea ice classification. It was observed that the de-speckled image obtained by the proposed method resulted in the most accurate classified map. An overall classification accuracy of about 79% was obtained by the proposed method, which was 11%, 15%, and 18% higher than the enhanced Lee method, the Nonlocal Means and Refined Lee method, and the Kuan method, respectively. In summary, the results demonstrated the significance of an efficient de-speckling method for improving the quality of PolSAR image processing (e.g. sea ice classification).

## ACKNOWLEDGEMENT

This research was undertaken with financial support of the Newfoundland and Labrador Research and Development Corporation (RDC). The authors also thank Thomas J. McKeever of Statoil for helpful conversations directly relating to this project and past discussions that have supported the basis of this research. ALOS PALSAR-1 data is copyrighted JAXA and provided by Alaska Satellite Facility (ASF). Daily ice charts is provided by the Canadian Ice Service (CIS), Environment of Canada.

## REFERENCES


Argenti, F., Lapini, A., Bianchi, T. and Alparone, L., 2013. A tutorial on speckle reduction in synthetic aperture radar images. *IEEE Geoscience and remote sensing magazine*, *1*(3), pp.6-35.

Hamilton, J. and Wu, Y., 2013. *Synopsis and trends in the physical environment of Baffin Bay and Davis Strait*. Ocean and Ecosystem Sciences Division, Maritimes Region, Fisheries and Oceans Canada.

Karvonen, J., Simila, M. and Makynen, M., 2005. Open water detection from Baltic Sea ice Radarsat-1 SAR imagery. *IEEE Geoscience and Remote Sensing Letters*, *2*(3), pp.275-279.

Lee, J.S., Jurkevich, L., Dewaele, P., Wambacq, P. and Oosterlinck, A., 1994. Speckle filtering of synthetic aperture radar images: A review. *Remote Sensing Reviews*, *8*(4), pp.313-340.

Lopes, A., Nezry, E., Touzi, R. and Laur, H., 1993. Structure detection and statistical adaptive speckle filtering in SAR images. *International Journal of Remote Sensing*, *14*(9), pp.1735-1758.

Mahdianpari, M., Motagh, M. and Akbari, V., 2012, July. Speckle reduction and restoration of synthetic aperture radar data with an adoptive markov random field model. In *Geoscience and Remote Sensing Symposium (IGARSS), 2012 IEEE International* (pp. 1-4). IEEE.

Novak, L.M. and Burl, M.C., 1990. Optimal speckle reduction in polarimetric SAR imagery. *IEEE Transactions on Aerospace and Electronic Systems*, *26*(2), pp.293-305.

Ochilov, S. and Clausi, D.A., 2012. Operational SAR sea-ice image classification. *IEEE Transactions on Geoscience and Remote Sensing*, *50*(11), pp.4397-4408.

Richards, J.A. and Richards, J.A., 1999. *Remote sensing digital image analysis* (Vol. 3). Berlin et al.: Springer.

Scheuchl, B., Cumming, I. and Hajnsek, I., 2005. Classification of fully polarimetric single-and dual-frequency SAR data of sea ice using the Wishart statistics. *Canadian Journal of Remote Sensing*, *31*(1), pp.61-72.

Touzi, R., 2002. A review of speckle filtering in the context of estimation theory. *IEEE Transactions on Geoscience and Remote Sensing*, *40*(11), pp.2392-2404.

Xie, H., Pierce, L.E. and Ulaby, F.T., 2002. SAR speckle reduction using wavelet denoising and Markov random field modeling. *IEEE Transactions on geoscience and remote sensing*, *40*(10), pp.2196-2212.